Global Biogeochemical Cycles

RESEARCH ARTICLE
10.1029/2020GB006698

Global N_2O Emissions From Cropland Driven by Nitrogen Addition and Environmental Factors: Comparison and Uncertainty Analysis

Rongting Xu[1], Hanqin Tian[1], Shufen Pan[1], Stephen A. Prior[2], Yucheng Feng[3], and Shree R. S. Dangal[4,1]

[1]International Center for Climate and Global Change Research, School of Forestry and Wildlife Sciences, Auburn University, Auburn, AL, USA, [2]USDA-ARS National Soil Dynamics Laboratory, Auburn, AL, USA, [3]Department of Crop, Soil and Environmental Sciences, Auburn University, Auburn, AL, USA, [4]Woodwell Climate Research Center, Falmouth, MA, USA

Key Points:
- Synthetic N fertilizer contributed to N_2O emissions of 2.0 ± 0.1 Tg N year^{-1} from global cropland between 2000 and 2014
- Uncertainty remains in fertilizer-induced N_2O emissions due to temporal and spatial differences in current N fertilizer data sets
- Changes in environmental factors increased cropland N_2O emissions; however, the magnitude of environmental effects remain highly uncertain

Supporting Information:
- Supporting Information S1

Correspondence to:
H. Tian,
tianhan@auburn.edu

Citation:
Xu, R., Tian, H., Pan, S., Prior, S. A., Feng, Y., & Dangal, S. R. S. (2020). Global N_2O emissions from cropland driven by nitrogen addition and environmental factors: Comparison and uncertainty analysis. *Global Biogeochemical Cycles*, *34*, e2020GB006698. https://doi.org/10.1029/2020GB006698

Received 4 JUN 2020
Accepted 9 NOV 2020
Accepted article online 12 NOV 2020

Abstract Human activities have caused considerable perturbations of the nitrogen (N) cycle, leading to a ~20% increase in the concentration of atmospheric nitrous oxide (N_2O) since the preindustrial era. While substantial efforts have been made to quantify global and regional N_2O emissions from cropland, there is large uncertainty regarding how climate change and variability have altered net N_2O fluxes at annual and decadal time scales. Herein, we applied a process-based dynamic land ecosystem model (DLEM) to estimate global N_2O emissions from cropland driven by synthetic N fertilizer application and multiple environmental factors (i.e., elevated CO_2, atmospheric N deposition, and climate change). We estimate that global cropland N_2O emissions increased by 180% (from 1.1 ± 0.2 to 3.3 ± 0.1 Tg N year^{-1}; mean ±1 standard deviation) during 1961–2014. Synthetic N fertilizer applications accounted for ~70% of total emissions during 2000–2014. At the regional scale, Europe and North America were two leading regions for N_2O emissions in the 1960s. However, East Asia became the largest emitter after the 1990s. Compared with estimates based on linear and nonlinear emission factors, our results were 150% and 186% larger, respectively, at the global scale during 2000–2014. Our higher estimates of N_2O emissions could be attributable to the legacy effect from previous N addition to cropland as well as the interactive effect of N addition and climate change. To reduce future cropland N_2O emissions, effective mitigation strategies should be implemented in regions that have received high levels of N fertilizer and regions that would be more vulnerable to future climate change.

1. Introduction

The accumulation of terrestrial biogenic methane (CH_4) and nitrous oxide (N_2O) induced by anthropogenic activities has offset the cooling effect due to carbon dioxide (CO_2) uptake by plants, resulting in a net warming effect on the climate system (Tian et al., 2016). The warming potential of N_2O is 265–298 times higher than CO_2 on a 100-year timescale (Ciais et al., 2013; Myhre et al., 2013). In addition, N_2O resides in the atmosphere for 116 ± 9 years and is also a reactant that can deplete stratospheric ozone (Nevison & Holland, 1997; Prather et al., 2015). Compared to the preindustrial era, atmospheric N_2O concentration has increased from 275 to 331 parts per billion (ppb) as of 2018 (Hall et al., 2007; Prinn et al., 2018). Recently, the Global N_2O Model Inter-comparison Project (NMIP, Tian et al., 2019) reported that global soil N_2O emissions have increased from 6.3 ± 1.1 Tg N year^{-1} in the preindustrial period to 10.0 ± 2.0 Tg N year^{-1} over the period of 2007–2016.

As of 2010, human-induced inputs of reactive nitrogen (Nr) were at least two times larger than naturally fixed N (Ciais et al., 2013). Reactive N production increased from approximately 15 Tg N year^{-1} (Tg = 10^{12} g) in 1900 to 156 Tg N year^{-1} in 1995 and further increased to 187 Tg N year^{-1} in 2005 (Galloway et al., 2008). Due to rapid Nr increases from different sources (e.g., agriculture, industry, and biomass burning), anthropogenic N_2O emissions have grown steadily and were estimated to be 6.9 Tg N year^{-1} (ranging from 2.7 to 11.1) in 2006 (Ciais et al., 2013; Reay et al., 2012). Among increased anthropogenic N_2O emissions, agricultural activities are the dominant source due to widespread synthetic N fertilizer and manure usage in croplands (Davidson, 2009; Reay et al., 2012; Syakila & Kroeze, 2011;

Tian, Xu, Canadell, et al., 2020). Between 2001 and 2011, annual N_2O emissions from synthetic fertilizer increased by 37% based on data from the Food and Agriculture Organization Corporate Statistical Database (FAOSTAT) (Gerber et al., 2016). Tremendous efforts have been made to estimate global and regional N_2O emissions from agricultural systems; however, the proportion of N_2O emissions associated with fertilizer remains largely uncertain (Davidson, 2009; Tian et al., 2018, 2019). In NMIP simulations, synthetic N fertilizer contributed 2.0 $\pm$ 0.8 Tg N year^{-1} and accounted for 54% of increased terrestrial N_2O emissions during 2007–2016 relative to the preindustrial period (Tian et al., 2019). However, different estimates with large uncertainty ranges also appeared in other studies (Crutzen et al., 2016; Davidson, 2009; Gerber et al., 2016; Mosier et al., 1998; Reay et al., 2012; Saikawa et al., 2014). Large uncertainties of these estimates were associated with approaches used to identify and quantify globally important sources of N_2O (Davidson, 2009). The two main approaches were bottom-up (inventory, statistical extrapolation of local flux measurements, and process-based modeling) and top-down (atmospheric inversion) methodologies (Davidson & Kanter, 2014; Tian et al., 2016). For example, Tian et al. (2016) synthesized estimates of global N_2O fluxes derived from different top-down and bottom-up studies for agriculture and waste during 1981–2010. Their results indicated that estimates from bottom-up methods (4.6 $\pm$ 0.2, 5.5 $\pm$ 0.7 Tg N year^{-1}) were much higher than top-down estimates (4.1 $\pm$ 0.6, 4.4 $\pm$ 0.6 Tg N year^{-1}) in the 1990s and 2000s.

Emission factors (EFs), which vary in different sectors of N_2O emission sources, were developed by the Intergovernmental Panel on Climate Change (IPCC) as a common means to evaluate emissions at country scales and were applied to develop several bottom-up inventories (e.g., Emission Database for Global Atmospheric Research [EDGAR; Olivier et al., 2002], Global Emission Inventory Activity [GEIA, http://www.geiacenter.org/], and FAOSTAT [http://www.fao.org/faostat/en/]). However, it should be noted that there are large uncertainties in these N_2O emission estimates when default EFs are applied at national or global scales (Crutzen et al., 2016; Davidson, 2009; Smith et al., 2012). Ground-based observations are an important approach to estimate N_2O emissions from specific sites, which could provide relatively accurate estimates for developing EFs models and validating results from process-based models (Rapson & Dacres, 2014). In addition, process-based models are essential tools in assessing and predicting feedbacks of terrestrial ecosystems related to climate change (Reynolds & Acock, 1997; Tian et al., 2019). Nitrous oxide is biologically produced in soils during denitrification and nitrification (Wrage-Mönnig et al., 2018); these processes are mainly driven by soil conditions, such as soil temperature, moisture content, pH, and substrate availability (mineral N and organic C) (Brotto et al., 2015; Butterbach-Bahl et al., 2013; Firestone & Davidson, 1989; Goldberg & Gebauer, 2009; Rowlings et al., 2015), as well as human management practices such as synthetic N fertilizer, manure application, irrigation, and tillage (Cai et al., 1997; Ding et al., 2010; Rice & Smith, 1982). Compared to constant EFs in the IPCC guidelines, process-based models are necessary for their capability to study spatiotemporal variability of N_2O emissions under changing circumstances such as environmental factors and management practices in global croplands.

Previous studies mainly focused on estimating N_2O emissions from synthetic fertilizer or manure applications through EFs regardless of environmental factors (Gerber et al., 2016; Shcherbak et al., 2014; Yan et al., 2003), or based on statistical models (Bouwman et al., 2002; Davidson, 2009; Wang et al., 2020; Zhou et al., 2015). Large uncertainties remain in understanding how annual and decadal climate change and variability affected N_2O emissions from croplands at global and regional scales. In addition, several newly developed spatial data sets of synthetic N fertilizer application in cropland published in the past decade can be used to examine its impact on cropland N_2O emissions. In this study, we applied the Dynamic Land Ecosystem Model (DLEM, Tian et al., 2011) to investigate long-term N_2O emissions at global and sectoral scales driven by environmental factors and N inputs during 1961–2014. The objectives of this study were to (1) provide a time-series estimate of N_2O emissions from global cropland; (2) examine spatial variability of cropland N_2O emissions during 1961–2014; (3) attribute factorial contributions to increases in N_2O emissions; and (4) investigate uncertainties associated with various N input data sets. The global change factors evaluated in this study included climate change and variability, elevated atmospheric CO_2 concentration, atmospheric N deposition, and fertilizer N application in croplands.

2. Materials and Methods

2.1. Model Description

DLEM was designed to track key biological processes of CO_2, CH_4, N_2O, and NO production and their exchange between the terrestrial ecosystem and atmosphere at time steps ranging from daily to yearly (Tian et al., 2011). DLEM is characterized by cohort structure, multiple soil layer processes, coupled C, water, and N cycles, enhanced land surface processes, and dynamic linkages between terrestrial and riverine ecosystems. In DLEM, the cycles of C, N, and water are fully coupled for simulating the hydrological, biogeochemical fluxes, and pool sizes at multiple scales in space from site to region to globe (Tao et al., 2014). Nitrogen is essential in all biological processes of DLEM simulations. It exchanges between land ecosystem and its surroundings through deposition, leaching and runoff, N-containing gas emissions as well as harvest. Available N changes in DLEM rely on the difference between N inputs (i.e., N deposition, fertilization and biological N fixation) and N outputs (i.e., N leaching and runoff, N_2O, NO, and N_2 emissions, and NH_3 volatilization). The effluxes of N are also influenced by environmental factors, such as temperature, moisture, and soil properties. Forms of reactive N in DLEM include organic N stored in biomass, labile N stored in plants, organic N stored in soils and litter/woody debris, dissolved soil organic N, and soil inorganic N (Lu & Tian, 2013; Tian, Xu, Pan, et al., 2020. Our previous work has shown a detailed description of trace gas modules (Dangal et al., 2019; Lu & Tian, 2013; Tian et al., 2010; Xu et al., 2017; Zhang et al., 2016), biological processes of crops and plants (i.e., photosynthesis and evapotranspiration) (Pan et al., 2014, 2015), biogeochemical processes in soils (i.e., nitrification, denitrification, and decomposition) (Xu et al., 2017; Yang et al., 2015), and agricultural managements in the DLEM agricultural module (Ren et al., 2011, 2020; Tian et al., 2012; Xu et al., 2018, 2019; Zhang et al., 2018).

2.2. Input Data

Data sets used to simulate cropland N_2O emissions included (i) environmental factors such as climate, atmospheric CO_2 concentration, and atmospheric N deposition; (ii) topography and soil properties; and (iii) dynamic cropland distribution maps and land management practices (i.e., synthetic N fertilizer application, irrigation, rotation, harvest, and crop residue return). All input data sets for driving model simulations in this study were at a spatial resolution of 0.5° × 0.5° latitude/longitude. This study included biological N fixation by crops but excluded manure N inputs in cropland.

Climate data were a fusion of Climatic Research Unit (CRU) and NCEP/NCAR reanalyzed data sets (version 7) at the global scale between 1901 and 2014. The time-series climate data showed large interannual variations, while an overall increasing trend of annual temperature and precipitation was found during 1961–2014 (Figure S1a in the Supporting Information). The monthly CO_2 concentration data set was obtained from National Oceanic and Atmospheric Administration (NOAA) extended GLOBALVIEW-CO_2 (http://www.esrl.noaa.gov/gmd/ccgg/globalview/co2/), spanning from 1900–2015. Atmospheric CO_2 concentration increased from 319 ppm to 398 ppm at a rate of 1.5 ppm year^{-1} (Figure S1b). We obtained two sets of atmospheric N deposition data (i) from the atmospheric chemistry transport model (Wei et al., 2014) that provided NH_x-N and NO_y-N deposition rates with interannual variations constrained by EDGAR-HYDE N emission data (van Aardenne et al., 2001) and (ii) from the International Global Atmospheric Chemistry (IGAC)/Stratospheric Processes and Their Role in Climate (SPARC) Chemistry–Climate Model Initiative (CCMI) N deposition fields (Eyring et al., 2013). The former data set grew continuously at a rate of 0.76 Tg N year^{-2} ($R^2 = 0.99$), while the latter increased at a faster rate of 1.1 Tg N year^{-2} ($R^2 = 0.99$) between 1961 and 1990 but stabilized thereafter until 2014 (Figure S2a).

Elevation, slope, and aspect were derived from global 30 arc-second elevation products (GTOPO30; https://lta.cr.usgs.gov/GTOPO30), and soil texture was derived from the FAO Soil Database System (Reynolds et al., 2000). The spatial distribution of major crop types was identified according to the global crop geographic distribution map at 5′ × 5′ resolution (Leff et al., 2004) and the country-level FAOSTAT agricultural census as well as the regional-level census for China and India (Banger et al., 2015; Ren et al., 2011). Global irrigation distribution was developed by incorporating a global irrigation map, a historical gridded crop distribution map, and agricultural census (Ren et al., 2020). We assumed that the irrigation treatment was conducted in irrigated dry farmland and paddy fields and that the irrigation date was the point when soil moisture of the top layer dropped to 30% of maximum available water (i.e., field capacity minus wilting

point) during the growing season (Ren et al., 2011; Zhang et al., 2016). Our study included 10 major crop types (i.e., rice, corn, wheat, soybean, cotton, millet, sorghum, groundnuts, barley, and rapeseed) and different crop rotation systems (e.g., rice-wheat, rice-rice, corn-wheat, and soybean-wheat). Fertilizer timings were determined based on previous literature (see Supporting Information Appendix S1 in Xu et al., 2018 and Supporting Information Appendix S2 and Table S1 in Xu et al., 2019).

We obtained three spatially explicit time-series data sets of synthetic N fertilizer use at a resolution of 0.5° × 0.5° latitude/longitude from (i) Lu and Tian (2017), (ii) Nishina et al. (2017), and (iii) Zaehle et al. (2011). Lu and Tian (2017) developed the data sets through spatializing IFA-based country-level N fertilizer consumption amount according to crop specific N fertilizer application rates, distribution of crop types, and historical cropland distribution during 1960–2013. Nishina et al. (2017) generated data sets by incorporating country-level annual total N fertilizer consumption and fraction of NH_4^+ (and NO_3^-) in N fertilizer inputs from FAOSTAT during 1960–2010. Zaehle et al. (2011) developed their data set based on country-level annual N fertilizer use from FAOSTAT during 1961–2005. All above-mentioned data sets assumed that country-level synthetic N fertilizer amounts obtained from FAOSTAT were applied to croplands rather than agricultural systems (croplands and pastures). Based on country-scale data of N fertilizer application to pastures (Lassaletta et al., 2014), we separated cropland N fertilizer application from pastures in these three N fertilizer data sets. Since data provided by Lassaletta et al. (2014) was from 1960 to 2009, we assumed that there was no N fertilizer used in pastures before 1960 and that applications of N to pastures during 2010–2014 remained similar to 2009. Three data sets showed high consistence in temporal trends and in magnitudes at the global scale but diverged in spatial patterns over the period of 1961–2014. This difference between three data sets was attributable to different methodologies and different land use data sets that were used. Synthetic N fertilizer application in global cropland increased from 12 ± 1.0 Tg N $year^{-1}$ (mean ±1 standard deviation) in 1961 to 108 Tg N $year^{-1}$ in 2014 at an average rate of 1.7 Tg N $year^{-2}$ ($R^2 = 0.97$) (Figure S2b). In 1961, all three data sets showed consistently higher N inputs in Europe than the rest of world, however, with an obvious divergence in spatial patterns in the United States: in Lu and Tian (2017), the spatial distribution was almost uniform with a hotspot detected in Wisconsin and Nebraska; in Nishina et al. (2017), a smaller N input was shown in the Midwest, but this pattern was reversed in Zaehle et al. (2011). In 2005, N inputs increased worldwide compared to 1961. However, spatial patterns in the three data sets differed considerably, especially in regions with a higher amount of N input such as Europe, India, China, and the United States (Figure S3).

In DLEM simulations, synthetic N fertilizer (units: grams of N per square meter of cropland; g N m^{-2}·cropland) was applied in each grid cell where cropland area was not equal to zero. We multiplied cropland area (units: m^2) by cropland N_2O emissions (g N m^{-2}·cropland) in each grid cell after model simulations were finished and summed up gridded emissions to obtain the global total N_2O emission during 1961–2014. Cropland distribution data sets at a spatial resolution of 0.5° developed by aggregating the 5′ resolution History Database of the Global Environment (HYDE v3.2) global cropland distribution data during 1860–2016 (Klein Goldewijk et al., 2017) were used to develop gridded data sets of fertilizer N application rates in Lu and Tian (2017) The cropland distribution data set at a resolution of 0.5° × 0.5° used to generate N fertilizer application rates in Nishina et al. (2017) and Zaehle et al. (2011) was obtained from the Harmonized Global Land Use map (LUHa) v1.0 for 1860–2005 (Hurtt et al., 2011) that was adapted from HYDE v3.1 (Klein Goldewijk et al., 2010).

2.3. Experimental Design

Implementation of DLEM simulations included three steps: (1) equilibrium run; (2) spin-up run; and (3) transient run. In the first stage of the DLEM simulation, we applied long-term mean climate data from 1901 to 1920 and other data sets in 1900 as inputs (including CO_2 concentration and N deposition) to run the model to reach an equilibrium state. The equilibrium state was assumed to be reached when interannual variations of C, N, and water storage were less than 0.1 g C m^{-2}, 0.1 g N m^{-2}, and 0.1 mm, respectively, during two consecutive 50 years. After this stage, the model was spun up driven by detrended climate data (1901 to 1920) to eliminate system fluctuations due to model shifting from equilibrium to transient runs (i.e., three spins with 20-year climate data each time). Finally, the model was run in transient mode. At this stage, seven simulation experiments were designed to evaluate N_2O emissions under various scenarios to identify contributions of environmental factors (Table 1).

Table 1
Design of Simulation Experiments

Experiment	Climate	CO_2	Atmospheric N deposition	Synthetic N fertilizer
Reference (S0)	1900	1900	1900	1900
All Combined (S1)[a]	1901–2014	1901–2014	1901–2014	1901–2014
No Climate (S2)	1900	1901–2014	1901–2014	1901–2014
No CO_2 (S3)	1901–2014	1900	1901–2014	1901–2014
No atmospheric N deposition (S4)	1901–2014	1901–2014	1900	1901–2014
No synthetic N fertilizer (S5)	1901–2014	1901–2014	1901–2014	1900

[a]Experiments designed to study impacts of three different fertilizer data sets and two different N deposition data sets in global croplands on N_2O emissions are included in S1 simulations: S1–1: Synthetic N fertilizer use from Lu and Tian (2017); S1–2: Synthetic N fertilizer use from Nishina et al. (2017); S1–3: Synthetic N fertilizer use from Zaehle et al. (2011); S1–4: Atmospheric N deposition from Wei et al. (2014); and S1–5: Atmospheric N deposition from CCMI

The DLEM simulation was from 1901 to 2014. However, in this study, we mainly focused on analyses of the period when N fertilizer use became widespread (i.e., 1961–2014). In the reference run (S0), all driving forces were kept at the 1900 level to track model drift and internal fluctuations, which provided background N_2O emissions with little human perturbation. All essential data sets were considered as inputs in the all combined runs (S1), which can provide N_2O emissions due to human management and changing environmental factors. In the remaining simulations (S2–S5), temporal changes of input factors were included, while one specific factor was set at the 1900 level. The difference between S1 and any simulation in S2–S5 represents the factorial impact on N_2O emissions during 1901–2014 (Table 1). For example, "No climate" (S2; all combined without climate change) had climate data kept constant at the 1900 level while all other factors changed. The difference between S1 and S2 represents the impact of climate change and its interactions with other environmental changes on N_2O emissions. The overall change induced by four factors was the difference between S1 and S0 simulations (defined as ΔN_2O_{all}). The change associated with each factor was defined as $\Delta N_2O_{factori.}$ The relative contribution (%) of each factor to the overall change in N_2O emissions was described as $\Delta N_2O_{factori}/\Delta N_2O_{all}$, and the interactive effect was calculated as $(\Delta N_2O_{all} - \Sigma\Delta N_2O_{factori})/\Delta N_2O_{all}$.

3. Results

3.1. Model Performance Evaluation

In situ observations were selected to evaluate model performance in modeling N_2O emissions in response to multiple N fertilizer addition levels for rice, wheat, corn, barley, soybean, cotton, sorghum, and pearl millet (Table S1). Overall, there was general agreement and strong correlation between observed and modeled N_2O emissions for three major crops (i.e., rice, wheat, and corn). In addition, we observed a roughly rising trend of N_2O emissions with increased synthetic N fertilizer application in both observations and simulations at site level. However, there was a large range of observed and modeled N_2O emissions from the control experiments with no N addition for these three crops at different sites (Figure 1). For example, observed wheat emissions varied from 0.1 to 2.17 kg N ha^{-1} compared to a range of 0.15 to 0.83 kg N ha^{-1} in modeled results. In addition, both observed and modeled N_2O emissions varied considerably at different levels of synthetic N fertilizer application (Figure 1). For example, observed corn N_2O emissions were as high as 5.13 ± 0.94 kg N ha^{-1} when receiving synthetic N fertilizer at 291 kg N ha^{-1}, while the modeled value was 4.63 ± 1.3 kg N ha^{-1}. Overall, there was a large difference between observed and modeled N_2O in response to N addition at some sites for all three crops (Figure 1). For instance, when corn received synthetic N fertilizer at 250 kg N ha^{-1}, N_2O emission was 5.10 ± 0.73 kg N ha^{-1} in our simulation compared to 1.07 ± 0.6 kg N ha^{-1} for field observation. In contrast, another corn site receiving synthetic N fertilizer at 250 kg N ha^{-1} had observed N_2O emissions of 3.89 ± 2.07 kg N ha^{-1} compared to simulated results of 1.71 kg N ha^{-1}.

3.2. Temporal Patterns of N_2O Emissions From Global Cropland During 1961–2014

Background emissions represent N_2O emissions from global cropland regardless of impacts induced by all factors and were kept constant (~0.4 Tg N $year^{-1}$ from the S0 simulation) during 1961–2014. Overall, N_2O

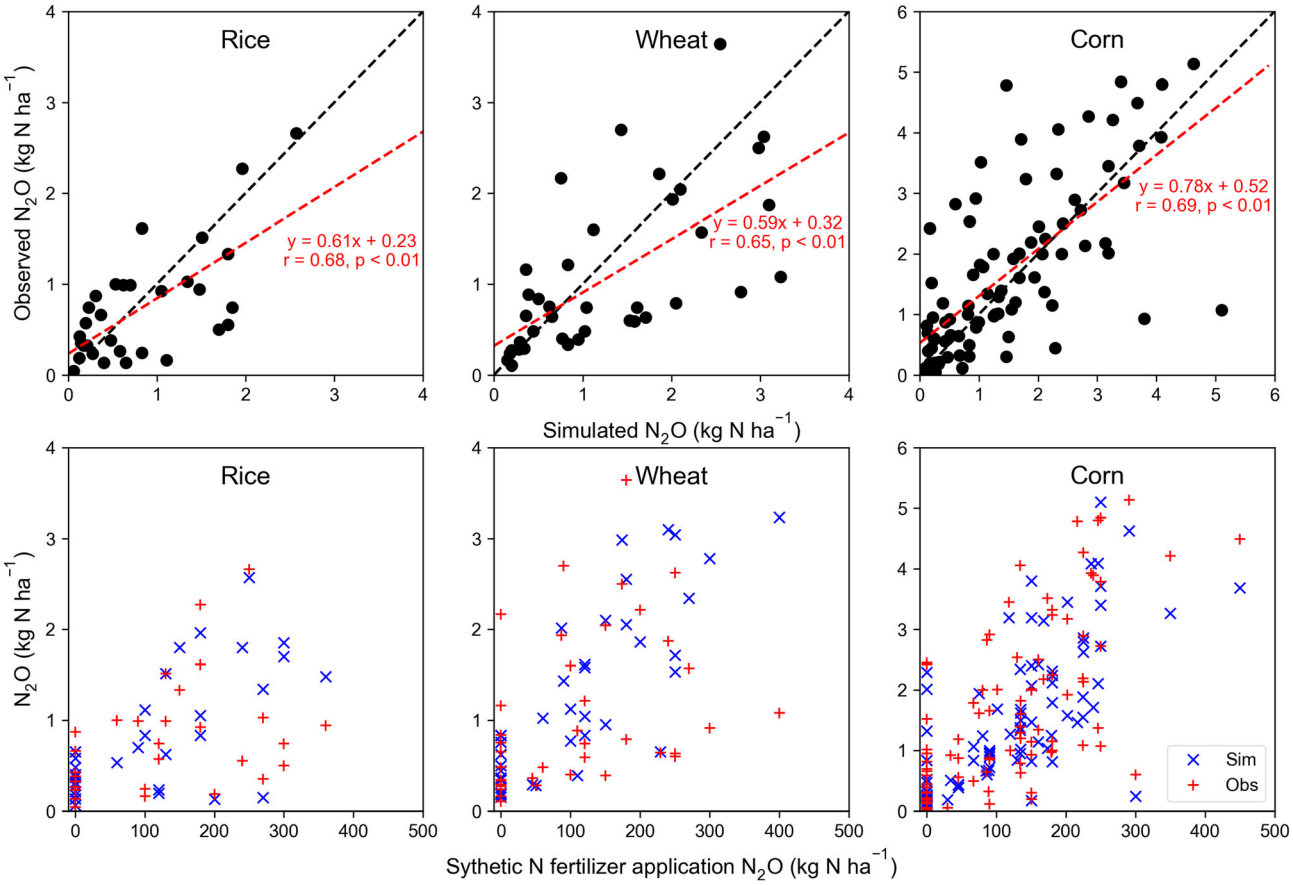

Figure 1. Comparison of observed and simulated N_2O emissions in response to different levels of synthetic N fertilizer for rice, wheat, and corn. In the lower three panels, blue "×" represents model simulated N_2O emissions, while red "+" represents observed N_2O emissions previously reported in the literature. The information on site location, synthetic N fertilizer application rate, year, and N_2O values can be found in Table S1.

emissions from global cropland showed a rapid increasing trend since 1961 (Figure 2). Cropland N_2O emissions increased by 185% between 2000 and 2014 compared to the 1960s. Global N_2O emissions increased from 1.0 ± 0.2 to 2.6 ± 0.1 Tg N year^{-1} at a rate of 0.07 Tg N year^{-2} (R^2 = 0.99) during 1961–1990. This was followed by a slight increase from 2.6 ± 0.1 to 3.2 ± 0.1 at a rate of 0.03 Tg N year^{-2} (R^2 = 0.90) during 1991–2014.

We partitioned the Earth land surface into 11 regions: Africa, South America, North America, Europe, North Asia, Oceania, South Asia, East Asia, West Asia, Central Asia, and Southeast Asia (Figure 3). Europe and North America were two leading continents for N_2O emissions and contributed 57% of the global total emission in the 1960s, followed by South America, East Asia, and South Asia. In total, East Asia and South Asia contributed less than 20% of the global total emission. Nitrous oxide emissions from North America and Europe showed a slight increase between 1960 and 1989, with an obvious decrease found in Europe after the 1980s. A slight decrease was also noted in North and Central Asia during 1980–2014. All remaining regions showed a fast-growing trend of N_2O emissions since the 1960s, especially South Asia and East Asia. During 2000–2014, however, N_2O emissions in both regions (i.e., South Asia and East Asia) accounted for 37% of total emissions, which was roughly equivalent to contributions from both North America and Europe (38%).

3.3. Spatial Patterns of N_2O Emissions From Global Croplands During 1961–2014

The spatial pattern of N_2O emissions showed large discrepancies in the past five decades (Figure 4). In the 1960s, N_2O emission rates as high as 0.25 g N m^{-2} year^{-1} were found in North America and Europe. In contrast, N_2O emission rates in most regions of East Asia and South Asia were as low as 0.04 g N m^{-2} year^{-1}.

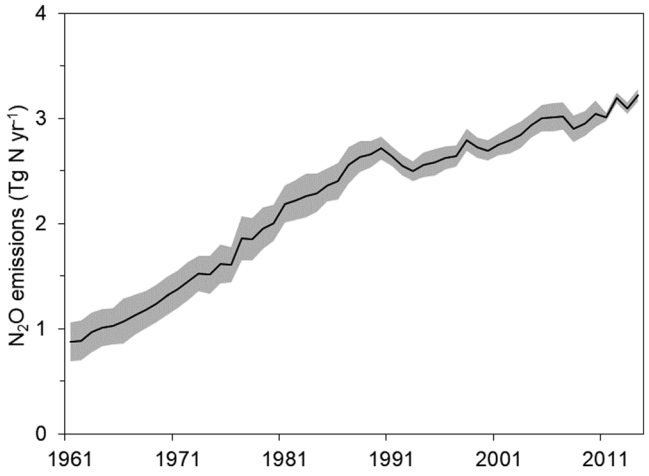

Figure 2. Annual total N_2O emissions from global cropland during 1961–2014. The uncertainty range was ±1 standard deviation from simulation results driven by different data sets of N inputs. Uncertainty of cropland N_2O emissions due to three different data sets of synthetic N fertilizer application covers the period 1961 to 2010. The smaller uncertainty range between 2011 and 2014 is due to using two different data sets of atmospheric N deposition without synthetic N fertilizer application data.

The North China Plain and central India showed slightly higher emission rates, which were still lower than 0.22 g N m^{-2} $year^{-1}$. Relatively higher emission rates were also found in Argentina in the 1960s. During 2000–2014, N_2O emission rates increased in most regions of the world. East Asia and South Asia showed a large increase in N_2O emission rates (higher than 0.35 g N m^{-2} $year^{-1}$), and a similar increase was also noted in North America, Europe, and West Asia.

3.4. Factorial Contributions of N_2O Emissions From Global Cropland

At the global scale, application of synthetic N fertilizer was a dominant factor (74%), while the other three factors shared a similar small contribution to the total emission increase in the past five decades. The interactive effect of four factors was positive and increased total N_2O emissions by ~13% (Figure 5). Climate variability exerted a large interannual variation in N_2O emissions (Figure S4), with a slightly increasing rate of 0.006 Tg N $year^{-2}$ (R^2 = 0.92) during 1961–2014. Rising atmospheric CO_2 concentration continuously accelerated N_2O emissions in global croplands, which was at an increasing rate of 0.008 Tg N $year^{-2}$ (R^2 = 0.90). Nitrogen deposition increased N_2O emissions at an average rate of 0.005 Tg N $year^{-2}$ (R^2 = 0.98) between 1961 and 1991 and showed a slower increase at a rate of 0.002 Tg N $year^{-2}$ (R^2 = 0.75) thereafter until 2014 (Figure S4). Global cropland N_2O emissions due to synthetic N fertilizer applications on average grew at a rate of 0.06 Tg N $year^{-2}$ (R^2 = 0.99) and 0.02 Tg N $year^{-2}$ (R^2 = 0.85) during 1961–1990 and 1991–2014, respectively (Figure S4).

From a regional perspective, N_2O emissions due to synthetic N fertilizer varied considerably during 1961–2014. East Asia, Europe, and North America were the top three regions accounting for fertilizer N-induced emissions during the past five decades. Europe and North Asia showed a declining trend of N_2O emissions after the 1980s, while all Asian regions (except for Central Asia) showed a rapid increasing trend since the 1960s. Asia (except for North Asia) accounted for 51% of global total emissions during 2000–2014. East Asia and South Asia were two dominant emitters contributing more than 82% of total

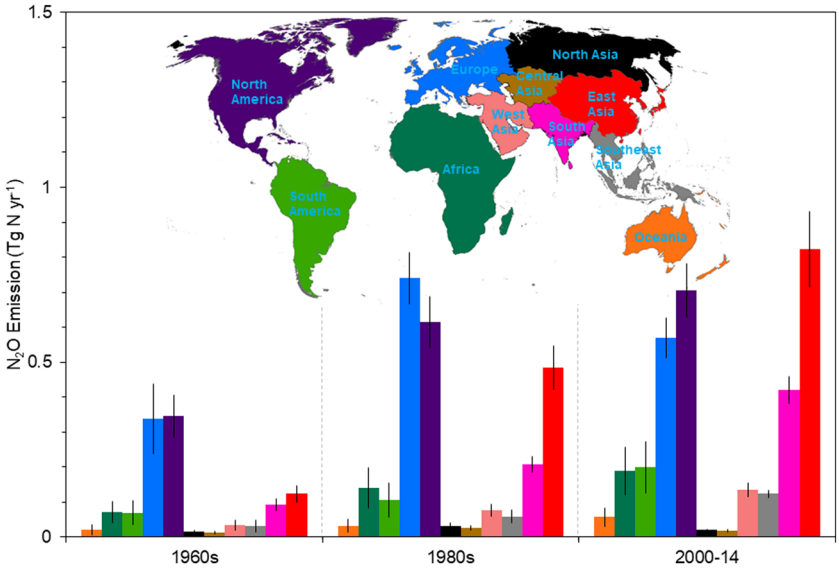

Figure 3. Decadal N_2O emissions at regional scales in the 1960s, 1980s, and 2000–2014. We included average N_2O emissions from all sources of N inputs with consideration of environmental effects. The uncertainty range was ±1 standard deviation from simulation results driven by different data sets of N input.

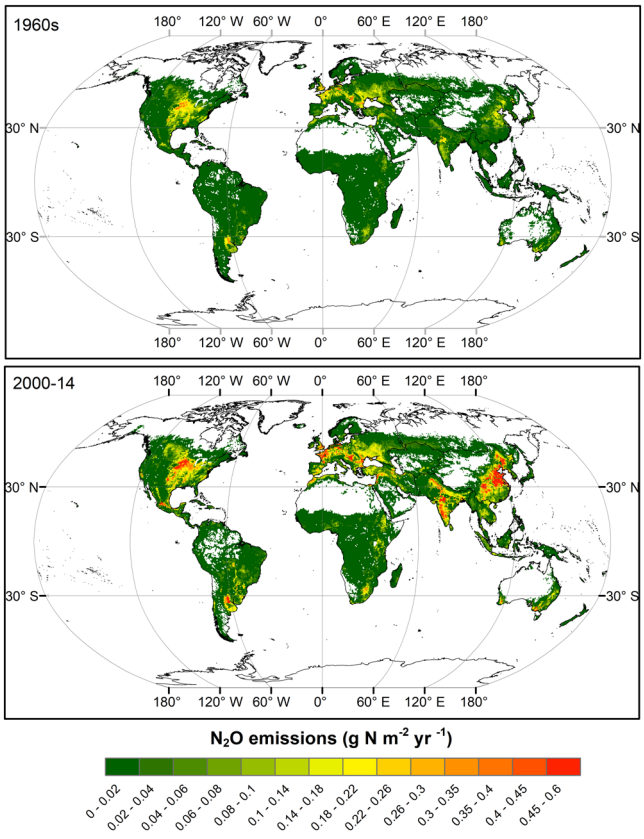

Figure 4. Spatial distributions of total N_2O emissions from global cropland in the 1960s and 2000–2014. We included average N_2O emissions from all sources of N inputs and environmental factors.

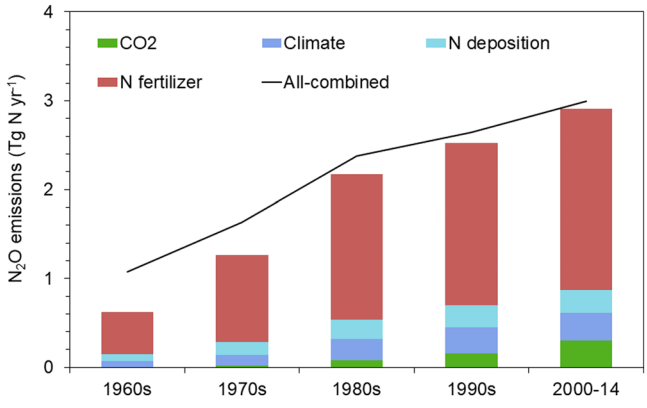

Figure 5. Relative contributions of driving factors to decadal N_2O emissions from global croplands. N_2O emissions attributed to fertilizer use and N deposition were based on average emission amounts from different N input data sets. The S1 experiment considered N_2O emissions changes induced by four factors. In counterfactual scenarios (S2—S5), we held one factor at the 1900 level while changing all other factors during 1901–2014. The all-combined line represents the overall change (i.e., difference between S1 and S0), which was not equal to the summed effects of counterfactual experiments due to interactive effects (see section 2.3).

emissions in Asia. Compared to the 1960s, N_2O emissions in five Asian regions (East, South, Southeast, West, and Central Asia) increased by 1,460% during 2000–2014 (Figure S5). Regional climate change substantially increased cropland N_2O emissions from North America and Europe despite large interannual variability during 1961–2014. In contrast, climate change slightly decreased emissions from South and Southeast Asia during 2004–2014 (Figure S6).

3.5. Uncertainty of N_2O Emissions From Different N Inputs

In our study, DLEM was driven by two data sets of atmospheric N deposition and three data sets of synthetic N fertilizer application in global cropland during 1961–2014. The difference in N_2O emissions induced by two atmospheric N deposition data sets from experiments S1-4 and S1-5 was relatively smaller at the global scale (~0.02 Tg N $year^{-1}$) for the period of 1961–2014. At the global scale, simulated N_2O emission from synthetic N fertilizer was highest (2.4 Tg N $year^{-1}$) for the S1-2 experiment, followed by 2.1 Tg N $year^{-1}$ for the S1-1 experiment during 1961–2010, and was least (2.0 Tg N $year^{-1}$) for the S1-3 experiment during 1961–2005. From a regional perspective, large uncertainties of N_2O emissions induced by synthetic N fertilizer remain in some regions (i.e., Europe, North America, South Asia, and East Asia) with higher amounts of N addition during 1961–2014 (Figures S5 and S7). Nitrous oxide emissions from European cropland from three model experiments (i.e., S1-1, S1-2, and S1-3) showed an obvious difference during 1960–1990. A relatively large uncertainty also exists for Africa, Southeast Asia, and South America that received much less N additions (Figures S5 and S7). Among the 11 regions, simulated N_2O emissions from African cropland soils were associated with the largest uncertainty, especially between 1970 and 2010 (Figure S7).

4. Discussion

4.1. Comparison With Previous Studies Based on EFs

Emission factors were one of the major approaches for estimating N_2O emissions from global and regional croplands in the past several decades. The widely used EFs in the IPCC 2006 Tier 1 Guideline were assumed to remain constant (0.3% for paddy rice, 1% for all other crops) for all countries across the globe. However, recent studies have argued that the IPCC approach underestimated direct emissions from global soils (Smith et al., 2012). Davidson (2009) provided an EF (2.5%) for N_2O emissions from synthetic N fertilizer based on the entire pattern of increasing N_2O concentrations since 1860 and his estimate including direct and indirect sources was 2.2 Tg N $year^{-1}$ in 2005. Our global estimate of synthetic N fertilizer induced direct N_2O emissions (2.1 $\pm$ 0.1 Tg N $year^{-1}$) with indirect emissions (~0.1 Tg N $year^{-1}$) from global rivers estimated by Yao et al. (2020) agreed with the estimate of Davidson (2009).

Recent studies including field experiments and meta-analysis indicated that EFs varied with N additions, cultivation practice, and environmental conditions (Shcherbak et al., 2014; Zhou et al., 2015). The 2019 refinement to IPCC 2006 Guidelines for National Greenhouse Gas Inventories also emphasized the role of climate in determining EF: the revised EFs in wet and dry climates are 1.6% and 0.5% of synthetic N inputs, respectively (IPCC, 2019). Shcherbak et al. (2014) found a

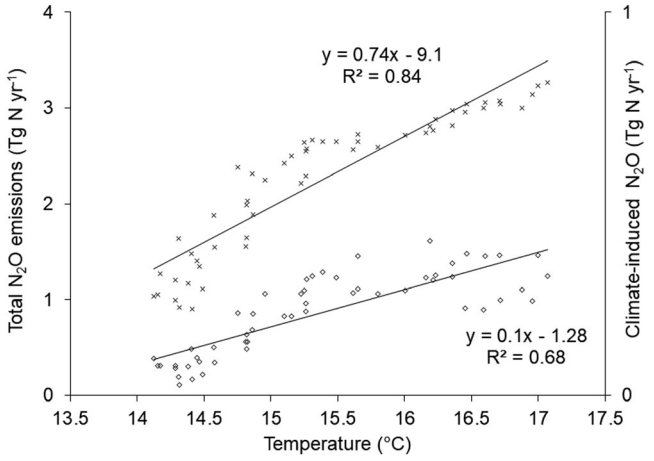

Figure 6. Cropland N_2O emissions response to global warming during 1961–2014. The correlation between average global annual cropland temperature and simulated N_2O emissions considering annual changes in the four factors (i.e., S1 experiment results; demonstrated as "×"), and the correlation between average global annual cropland temperature and simulated N_2O emissions due to the climate impact (i.e., S1 minus S2; demonstrated as "◇").

nonlinear response of N_2O emissions to N additions in most crops. The nonlinear response was also noted in a recent inversion-based estimate (Thompson et al., 2019). Gerber et al. (2016) applied linear (0.89%) and nonlinear EFs (0.77%) to compare fertilizer and manure N-induced N_2O emissions at global, country, and crop-type scales in 2000. Based on linear and nonlinear EFs provided in Gerber et al. (2016) and three N fertilizer application data sets, global emissions were calculated as 0.8 and 0.7 Tg N $year^{-1}$, respectively, during 2000–2014. Our results for synthetic N fertilizer (2.0 ± 0.1 Tg N $year^{-1}$) were 150% and 186% higher than estimates based on linear and nonlinear EFs, respectively, at the global scale during 2000–2014. Wang et al. (2020) reported a similar estimate (0.82 ± 0.34 Tg N $year^{-1}$) using a flux upscaling model (a statistical model-SRNM) evaluated by cross-validation with EF data from 180 globally distributed chamber-based N_2O flux observation sites. The estimated N_2O emissions by Wang et al. (2020) included N inputs (i.e., synthetic N-fertilizer, livestock manure, and crop residues applied to cropland) and environmental conditions (i.e., climate factors). Our higher estimates compared to statistical model-based estimates can be explained by the following two reasons. First, cropland N addition from previous years was possibly accumulated in soils and lost either through N gases (e.g., N_2O) or leaching/runoff, defined as "the legacy effect" (Tian, Xu, Canadell, et al., 2020) or "background" anthropogenic emissions (Wang et al., 2020). This effect is captured by the process-based terrestrial biosphere models, but not by two statistical models. For example, if we added "background" anthropogenic emissions (1.52 ± 0.16 Tg N $year^{-1}$, Kim et al., 2013) into the estimate from Wang et al. (2020), the summed value (2.35 ± 0.38 Tg N $year^{-1}$) was roughly comparable to 2.43 ± 0.31 Tg N $year^{-1}$ that was the sum of our estimate from synthetic N fertilizer (1.96 ± 0.16 Tg N $year^{-1}$) and the NMIP estimate (i.e., 0.47 ± 0.26 Tg N $year^{-1}$) from manure N application during 1990–2014. However, "background" anthropogenic emissions based on previous meta-analyses have large uncertainties due to limited data collection, and the estimated value could vary with climate change and land-use intensification (Kim et al., 2013). Second, warming may promote cropland N_2O emissions since (i) it can benefit crop growth and enhance root respiration; (ii) it can speed N mineralization; and (iii) it could directly stimulate the activity and abundance of denitrifers and nitrifiers (Li et al., 2020). Our modeled results indicate that warming could have accelerated soil nitrification and denitrification processes, resulting in increases in N_2O emissions with rising N addition to cropland soils (Figure 6; Pärn et al., 2018; Tian et al., 2019). Through comparisons to the aforementioned studies, the global total emission in this study is higher than the EF methodology and can serve as the upper boundary in assessing impacts of synthetic N fertilizer on N_2O emissions.

4.2. Comparison With NMIP Models

Results from the NMIP simulations were compared with our S1–S5 simulation since these two simulations were driven by the same data forcings. Our study included all factors considered in NMIP except for land cover change (LCC). The LCC effect on N_2O fluxes involves reduction due to the long-term effect of reduced mature forest area and emissions due to the post-deforestation pulse effect (Tian, Xu, Canadell, et al., 2020). However, we accounted for annual expansion of cropland area to guarantee the total amount of applied fertilizer during the study period. Since the LCC effect was not considered in our study, we subtracted this effect (i.e., SE4 and SE5) from NMIP SE2 simulations to make the comparison. There were six process-based terrestrial biosphere models in NMIP including DLEM (Tian et al., 2019). Here, we compared the DLEM simulation in this study with that in NMIP and found an identical result at the global scale (Figures S8 & S9). However, the magnitude of regional N_2O emissions was divergent. We observed 0.05 Tg N $year^{-1}$ and 0.04 Tg N $year^{-1}$ higher emission in North America and South America, respectively, with 0.09 Tg N $year^{-1}$ lower emission in Europe compared to DLEM results reported in NMIP between 1961 and 2014. Moreover, our estimate of DLEM-based N_2O emissions over East Asia and NMIP agreed well in

magnitude but diverged in interannual variability during 2004–2014. The regional emissions discrepancy was associated with different versions of climate data used to drive the DLEM model (Figures S10 and S11) as well as different experimental designs (Table 1 and Table 1 in Tian et al., 2019). For instance, N_2O emissions due to climate change were 10 times lower in NMIP than in our study. It is possible that the impact of climate change on N_2O emissions was enlarged from the interaction with increased cropland N addition (i.e., synthetic N fertilizer and atmospheric N deposition).

There remain large uncertainties in cropland N_2O emissions simulated by the six process-based terrestrial biosphere models at global and regional scales (Figures S8 and S9). Simulation results from the six models showed an increasing trend of global cropland N_2O emissions (but to divergent extents) between 1961 and 2014; similar highest emissions were from DLEM and VISIT, similar moderate emissions were from ORCHIDEE-CNP and OCN, and similar lowest emissions were from LPX-Bern and ORCHIDEE. The DLEM and VISIT models gave notably higher estimates for Europe, North America, East Asia, and South Asia, which collectively contributed over 80% of the global total cropland N_2O emissions estimated by both models. The ORCHIDEE-CNP and OCN models showed faster increases in emissions from Asian regions (East, South, and Southeast Asia) compared to other models, exceeding estimates from VISIT and DLEM models in the late 2000s. Although global estimates from ORCHIDEE and LPX-Bern models were consistent, regional emissions varied considerably. The ORCHIDEE model showed a high estimate for Europe and North Asia, while the LPX-Bern model showed high emissions for South America, South Asia, and East Asia. We observed a rising trend of N_2O emissions from all models in South Asia except for ORCHIDEE. In addition, four models showed faster increasing N_2O emissions in East Asia except for ORCHIDEE and LPX-Bern. The five models showed a similar pattern of interannual variability but to different degrees, whereas VISIT exhibited a different pattern of interannual variability to a larger extent. The difference in global cropland N_2O emissions between the six models is attributable to different model structure configurations and parameterization in cropland (Tian et al., 2018, 2019). For example, DLEM parameterized cropland processes by crop species, while crops in VISIT are grouped into paddy, generic C_3 crop (e.g., wheat), and warm C_4 crop (e.g., corn) (Tian et al., 2019). In addition, missing or simplified management practices (e.g., irrigation, tillage, and crop residue return) in models could cause large uncertainties in simulating cropland N_2O emissions. Therefore, improving model representation of key N_2O flux processes in cropland is of utmost importance.

4.3. Cropland N_2O Emissions From Different N Inputs

Previous studies have shown that N deposition could degrade aquatic ecosystems and human health and increase GHG emissions (Goulding et al., 1998; Xu et al., 2018, 2019; Yao et al., 2020). In this study, N deposition accounted for 8% of N_2O emissions over the contemporary period. Global N deposition-induced N_2O emission was highly correlated with the changing trend of N input data sets: a continuous increase of emissions driven by Wei et al. (2014); a faster increase between 1961 and 1990; and then a stabilization during 1991–2014 driven by Eyring et al. (2013). The difference between two estimates reached up to 0.08 Tg N $year^{-1}$ in 2014.

Global synthetic N fertilizer-induced N_2O emission was also correlated with tempo-spatial patterns and changes in N inputs. Due to different land use data sets and methodologies used to generate these three data sets (Lu & Tian, 2017; Nishina et al., 2017; Zaehle et al., 2011), spatial heterogeneity in N fertilizer use rates was obvious (Figure S3). The decreasing uncertainty of N_2O emissions between 1961 and 2008 is attributable to more consistence in magnitudes of these three N fertilizer data sets, while no uncertainty was reported between 2008 and 2014 since only Lu and Tian (2017) covered this time period (see Figure 2 and section 2.2). Concentrations of NH_4^+ and NO_3^- are significant factors that affect N_2O production in agricultural soils since they are necessary substrates for activities of denitrifiers and nitrifiers. The ratio of NH_4^+ to NO_3^- varied with different N fertilizer types. In DLEM simulations, this ratio was set constant when the N fertilizer was applied to cropland. In contrast, Nishina et al. (2017) generated N fertilizer application data sets during 1961–2010 and indicated that the NH_4^+/NO_3^- ratio increased as urea consumption increased over the study period. Simulation results using their data sets were generally higher than results driven by N fertilizer data sets from Lu and Tian (2017) and Zaehle et al. (2011). Large uncertainties remain for cropland N_2O emissions from regions with higher synthetic N fertilizer applications (i.e., Europe, Africa, South Asia, and

Southeast Asia). Africa also showed a large uncertainty despite much smaller N_2O emissions from less N inputs (Figures S5 and S6). Since the application of synthetic N fertilizer is a dominant source for increased cropland N_2O emission, harmonization of existing data sets may be a better approach to reduce emission uncertainties due to N inputs.

4.4. Contributions of Multiple Environmental Factors on Changes in N_2O Emissions

When studying fertilizer N-induced N_2O emissions from cropland, impacts from environmental factors and management practices should be considered (Gerber et al., 2016; Stehfest & Bouwman, 2006) since these factors can impact soil conditions and processes that control N_2O emissions (Bouwman et al., 2002). The interannual variability of terrestrial N_2O flux is driven by climate (Zaehle et al., 2011). Environmental factors included in this study increased N_2O emissions but with different magnitudes. A quantitative assessment that synthesized the effect of elevated CO_2 on GHG emissions found that increased concentrations of atmospheric CO_2 stimulated N_2O emissions by 19% (Van Groenigen et al., 2011). Our study found that the impact of CO_2 on N_2O emissions was 0.3 Tg N $year^{-1}$ during 2000–2014 (increasing rate of 0.009 Tg N $year^{-2}$ with $R^2 = 0.96$ since 1961), which was significantly correlated with the accelerating increase of atmospheric CO_2 concentration. This impact contributed to an almost 10% increase in cropland N_2O emissions for the period of 2000–2014. The effect of CO_2 fertilization on N_2O emissions diverges among ecosystems with varied N limitation strength (Ri & Prentice, 2008). Zaehle et al. (2011) found that CO_2 fertilization diminished up to 0.5 Tg N $year^{-1}$ of global N_2O emissions from the terrestrial biosphere based on OCN model simulations during 1860–2005. A decline of agricultural N_2O emissions due to rising CO_2 concentration was also reported in Kanter et al. (2016) based on GFDL-LM3-N.1 model simulations. In contrast, using meta-analysis, Van Groenigen et al. (2011) found increased atmospheric CO_2 enhanced N_2O emissions from upland soils (natural and agricultural), which agreed with our modeled results in global cropland. It is possible that increased CO_2 enhances crop root biomass and then more labile C (energy source for denitrifiers) enters into soils, thus stimulating N_2O emissions from denitrification (Van Groenigen et al., 2011). In natural ecosystems, model results show that increased CO_2 decreases soil N_2O emissions through enhanced vegetation N uptake, possibly enhanced N use efficiency, and reduced soil inorganic N (Tian et al., 2019). However, it is a different story in fertilized cropland soils which usually contain sufficient N for crop uptake and for denitrifiers or nitrifiers use under increased CO_2 conditions, thus favoring N_2O production. Hence, magnitude of the CO_2 effect on N_2O emissions is still poorly understood at the global level. For example, only DLEM and ORCHIDEE in NMIP show that elevated CO_2 increased cropland N_2O emissions (Tian et al., 2019).

Global cropland surface temperature showed a continuous increase since 1961 despite considerable interannual variability (Figure S1a). Zaehle et al. (2011) reported that warming effects increased global N_2O emissions by 0.8 Tg N $year^{-1}$ from the terrestrial biosphere during 1860–2005. In our study, climate variability and change caused an increase of 0.3 Tg N $year^{-1}$ from global cropland during 2000–2014 (Figures 5 and 6). At the regional scale, climate change largely increased cropland N_2O emissions from North America and Europe during 1961–2014, which is possibly attributable to temperature increases in both regions (Figure S10a). A similar positive effect was found in NMIP models but with different magnitudes (Tian et al., 2019). Warming favors N_2O emissions because denitrifiers may adapt to higher temperature (Pärn et al., 2018). A recent meta-analysis found that temperature increased terrestrial N_2O emissions by 33% inclusive of all possible biomes across the globe. Regional climate change slightly decreased cropland N_2O emissions from South and Southeast Asia during 2004–2014 (Figure S6). This decrease might be associated with substantial precipitation increases in both regions (Figure S10b). For example, regional climate change in South Asia increased N_2O emissions in 2003, but thereafter emissions decreased (Figure S6). Such decreases occurred in agricultural areas with substantially increased rainfalls during 2004–2014 compared to the year 2003 (Figure S11). However, the N_2O decline in West Asia could be attributable to precipitation decreases during 1961–2014 (Figures S6 and S11). Soil moisture regulates N_2O emissions since it highly affects oxygen availability to soil microbes (Butterbach-Bahl et al., 2013). Soil water content that results in water-filled pore space (WFPS) less than 30% or larger than 80% can suppress N_2O production in soils (Davidson et al., 2000). Overall, elevated CO_2 and climate change led to increases in N_2O emissions from

global croplands during the past five decades. Merely applying an empirical EF may not catch the interannual variability and the legacy effect of N in N_2O emissions.

4.5. Uncertainties and Future Work

Uncertainty in model simulations is influenced by quality of input data, parameterization, and model structure configuration. Our study showed spatial heterogeneity of cropland N_2O emissions driven by three different data sets. Thus, further improvement of gridded synthetic N fertilizer data through joint community efforts is necessary to reduce simulation uncertainties. However, uncertainties from the six different NMIP models were much larger than that due to divergent sources of N inputs (i.e., synthetic fertilizer and atmospheric deposition). This indicates that improvements in model processes might be as important as improving the input data set for estimating global and regional cropland N_2O emissions. Cropland N_2O emission from animal manure application is a major contributor to increased total emissions (Bouwman et al., 2013; Davidson, 2009; Tian et al., 2019), and has been reported in NMIP (Tian et al., 2019). Manure-induced N_2O in NMIP was driven by a newly developed long-term data set of manure N application in global cropland (Zhang et al., 2017). Here, uncertainty in manure-induced N_2O emissions was not investigated since it is difficult to obtain other sets of long-term manure N application data to drive the DLEM. Such an effort should be undertaken in future investigations when multiple manure application data sets are available. In addition, other agronomic practices including irrigation, crop rotation, residue return to cropland, and natural disturbance (e.g., insect pests) are simplified in the current DLEM model. Our study treated synthetic N fertilizer as a total input for simulating cropland N_2O emissions and did not distinguish fertilizer type (Xu et al., 2019), which could lead to uncertainties in DLEM-based estimates. Although our site-level simulations generally agreed with observed N_2O emissions (Figure 1), there were positive or negative discrepancies between observed and simulated N_2O in response to difference levels of synthetic N fertilizer application. Theses discrepancies are possibly attributable to agronomic practices, climate conditions, soil properties, N leaching/runoff, and the amount of N retained in soils. In addition, these site-level differences could lead to simulation uncertainties at global and regional scales. Xu et al. (2017) identified and quantified five key parameters (i.e., maximum nitrification and denitrification rates, N fixation rate, and adsorption coefficients for soil NH_4^+ and NO_3^-) that dominated N_2O production and fluxes in pre-industrial soils. However, these factors were not considered in long-term runs of our model. Thus, our future work should include key parameters that affect N_2O flux calculations and different sets of input data. In addition, soil condition (specifically soil water content, oxygen, and pH) is a key factor that regulates the production and diffusion of N_2O in soils (Bouwman et al., 2002). Therefore, future work should also simulate cropland N_2O emissions through use of multiple sets of climate and irrigation data. Our study, NMIP simulations (Tian et al., 2019), and a recent meta-analysis (Li et al., 2020) show that temperature increased N_2O emissions. However, these warming-induced N_2O emissions were highly variable at global, regional, and biome scales. Moreover, LCC due to cropland expansion increased global cropland N_2O emissions by 0.7 ± 0.3 Tg N $year^{-1}$ during 2007–2016 (Tian et al., 2019). However, the LCC effect remains largely uncertain in different models where DLEM showed the highest LCC-induced emission (1.3 Tg N $year^{-1}$), while OCN showed the lowest emission (0.4 Tg N $year^{-1}$). Uncertainty in simulating LCC effects on cropland N_2O emissions could be reduced by improving model representations and validating models using more available site-level observations. "Background" anthropogenic emissions (legacy effect on soil N_2O emissions) are substantial and highly uncertain (Kim et al., 2013). Although the legacy effect was captured by process-based terrestrial biosphere models, it is difficult to quantify in our current model simulations. Quantification of legacy effects will be attempted in our future simulations. Moreover, more in situ experiments are needed to calibrate models to reduce model uncertainties.

5. Conclusions

Global food demand increase has boosted N_2O emissions to the atmosphere due to intensive agricultural N inputs by humans. A robust estimate of N_2O emissions from global croplands is vital for assessing environmental and human health impacts. Global N_2O emissions from agricultural systems showed an overall increasing trend with a rate of 0.06 Tg N $year^{-1}$ while its spatial pattern displayed large differences from 1961 to 2014. Although North America was a leading emitter in the 1960s, its emission has been surpassed

by Asia (particularly East Asia and South Asia) since the 1980s. During 2000–2014, the highest emitter among all regions was East Asia. Synthetic N fertilizer application was the major factor accounting for this substantial increase. On average, global N_2O emissions due to N fertilizer application increased from 0.3 ± 0.2 Tg N year^{-1} in 1961 to 2.2 Tg N year^{-1} in 2014. We also found that environmental factors including elevated CO_2, atmospheric N deposition, and climate change increased cropland N_2O emissions during 1961–2014. Moreover, climate variability explained the large interannual variation in N_2O emissions. Warming and elevated CO_2 continuously accelerated cropland N_2O emissions, while increases in N_2O due to atmospheric N deposition began to level off in the early 1990s. Cropland N_2O emissions induced by synthetic N fertilizer were highly correlated with tempo-spatial patterns and changes in N inputs. The large uncertainties of N_2O emissions in regions like Europe, Africa, South Asia, and Southeast Asia, were associated with three data sets of synthetic N fertilizer application. Our study using multiple data sources of N inputs in cropland showed a smaller uncertainty in N_2O emissions compared to uncertainty from six different process-based terrestrial biosphere models in NMIP. This discrepancy indicates that it is critical to improve model representation of key N_2O flux processes in cropland.

Acknowledgments
This research has been supported partially by NSF grant nos. 1903722 and 1243232; Andrew Carnegie Fellowship Award no. G-F-19-56910; NOAA grant nos. NA16NOS4780207 and NA16NOS4780204; and OUC-AU Joint Center Program. Statements made and views expressed are solely the responsibility of the authors. Model input and output data in this study are archived in International Center for Climate and Global Change Research at Auburn University (https://wp.auburn.edu/cgc/).

References

Banger, K., Tian, H., Tao, B., Lu, C., Ren, W., & Yang, J. (2015). Magnitude, spatiotemporal patterns, and controls for soil organic carbon stocks in India during 1901–2010. *Soil Science Society of America Journal*, *79*(3), 864–875. https://doi.org/10.2136/sssaj2014.11.0456

Bouwman, A., Boumans, L., & Batjes, N. (2002). Emissions of N_2O and NO from fertilized fields: Summary of available measurement data. *Global Biogeochemical Cycles*, *16*(4). https://doi.org/10.1029/2001GB001811

Bouwman, L., Goldewijk, K. K., Van Der Hoek, K. W., Beusen, A. H., Van Vuuren, D. P., Willems, J., et al. (2013). Exploring global changes in nitrogen and phosphorus cycles in agriculture induced by livestock production over the 1900–2050 period. *Proceedings of the National Academy of Sciences*, *110*(52), 20,882–20,887. https://doi.org/10.1073/pnas.1012878108

Brotto, A. C., Kligerman, D. C., Andrade, S. A., Ribeiro, R. P., Oliveira, J. L., Chandran, K., & de Mello, W. Z. (2015). Factors controlling nitrous oxide emissions from a full-scale activated sludge system in the tropics. *Environmental Science and Pollution Research*, 1–10. https://doi.org/10.1007/s11356-015-4467-x

Butterbach-Bahl, K., Baggs, E. M., Dannenmann, M., Kiese, R., & Zechmeister-Boltenstern, S. (2013). Nitrous oxide emissions from soils: How well do we understand the processes and their controls? *Philosophical Transactions of the Royal Society B*, *368*(1621), 20130122. https://doi.org/10.1098/rstb.2013.0122

Cai, Z., Xing, G., Yan, X., Xu, H., Tsuruta, H., Yagi, K., & Minami, K. (1997). Methane and nitrous oxide emissions from rice paddy fields as affected by nitrogen fertilisers and water management. *Plant and Soil*, *196*(1), 7–14. https://doi.org/10.1023/A:1004263405020

Ciais, P., Sabine, C., Bala, G., Bopp, L., Brovkin, V., Canadell, J., et al. (2013). Carbon and other biogeochemical cycles. In T. F. Stocker et al. (Eds.), *Climate change 2013: The physical science basis. Contribution of working group I to the Fifth Assessment Report of the Intergovernmental Panel on Climate Change* (pp. 465–570). Cambridge, UK and New York, NY, USA: Cambridge University Press.

Crutzen, P. J., Mosier, A. R., Smith, K. A., & Winiwarter, W. (2016). N_2O release from agro-biofuel production negates global warming reduction by replacing fossil fuels. In P. J. Crutzen & H. Brauch (Eds.), *Paul J. Crutzen: A pioneer on atmospheric chemistry and climate change in the Anthropocene. SpringerBriefs on pioneers in science and practice* (Vol. 50). Cham: Springer. https://doi.org/10.1007/978-3-319-27460-7_12

Dangal, S. R., Tian, H., Xu, R., Chang, J., Canadell, J. G., Ciais, P., et al. (2019). Global nitrous oxide emissions from pasturelands and rangelands: Magnitude, spatio-temporal patterns and attribution. *Global Biogeochemical Cycles*, *33*, 200–222. https://doi.org/10.1029/2018GB006091

Davidson, E. A. (2009). The contribution of manure and fertilizer nitrogen to atmospheric nitrous oxide since 1860. *Nature Geoscience*, *2*(9), 659–662. https://doi.org/10.1038/ngeo608

Davidson, E. A., & Kanter, D. (2014). Inventories and scenarios of nitrous oxide emissions. *Environmental Research Letters*, *9*(10), 105012. https://doi.org/10.1088/1748-9326/9/10/105012

Davidson, E. A., Keller, M., Erickson, H. E., Verchot, L. V., & Veldkamp, E. (2000). Testing a conceptual model of soil emissions of nitrous and nitric oxides: Using two functions based on soil nitrogen availability and soil water content, the hole-in-the-pipe model characterizes a large fraction of the observed variation of nitric oxide and nitrous oxide emissions from soils. *Bioscience*, *50*(8), 667–680. https://doi.org/10.1641/0006-3568(2000)050[0667:TACMOS]2.0.CO;2

Ding, W., Yagi, K., Cai, Z., & Han, F. (2010). Impact of long-term application of fertilizers on N_2O and NO production potential in an intensively cultivated sandy loam soil. *Water, Air, & Soil Pollution*, *212*(1–4), 141–153. https://doi.org/10.1007/s11270-010-0328-x

Eyring, V., Lamarque, J.-F., Hess, P., & Arfeuille, F. (2013). Overview of IGAC/SPARC chemistry-climate model initiative (CCMI) community simulations in support of upcoming ozone and climate assessments. *SPARC newsletter*, *40*(January), 48–66.

Firestone, M. K., & Davidson, E. A. (1989). Microbiological basis of NO and N_2O production and consumption in soil. In M. Andreae & O. D. S. Schimel (Eds.), *Exchange of trace gases between terrestrial ecosystems and the atmosphere* (pp. 7–21). New York: John Wiley.

Galloway, J. N., Townsend, A. R., Erisman, J. W., Bekunda, M., Cai, Z., Freney, J. R., et al. (2008). Transformation of the nitrogen cycle: Recent trends, questions, and potential solutions. *Science*, *320*(5878), 889–892. https://doi.org/10.1126/science.1136674

Gerber, J. S., Carlson, K. M., Makowski, D., Mueller, N. D., de Cortazar-Atauri, I. G., Havlík, P., et al. (2016). Spatially explicit estimates of N_2O emissions from croplands suggest climate mitigation opportunities from improved fertilizer management. *Global Change Biology*. https://doi.org/10.1111/gcb.13341

Goldberg, S. D., & Gebauer, G. (2009). Drought turns a Central European Norway spruce forest soil from an N_2O source to a transient N_2O sink. *Global Change Biology*, *15*(4), 850–860. https://doi.org/10.1111/j.1365-2486.2008.01752.x

Goulding, K., Bailey, N., Bradbury, N., Hargreaves, P., Howe, M., Murphy, D., et al. (1998). Nitrogen deposition and its contribution to nitrogen cycling and associated soil processes. *New Phytologist*, *139*(1), 49–58. https://doi.org/10.1046/j.1469-8137.1998.00182.x

Hall, B., Dutton, G., & Elkins, J. (2007). The NOAA nitrous oxide standard scale for atmospheric observations. *Journal of Geophysical Research*, *112*, D09305. https://doi.org/10.1029/2006JD007954

Hurtt, G., Chini, L. P., Frolking, S., Betts, R., Feddema, J., Fischer, G., et al. (2011). Harmonization of land-use scenarios for the period 1500–2100: 600 years of global gridded annual land-use transitions, wood harvest, and resulting secondary lands. *Climatic Change*, *109*(1–2), 117–161. https://doi.org/10.1007/s10584-011-0153-2

IPCC (2019). 2019 Refinement to the 2006 IPCC guidelines for national greenhouse gas inventories. In C. Buendia et al. (Eds.). Switzerland: IPCC.

Kanter, D. R., Zhang, X., Mauzerall, D. L., Malyshev, S., & Shevliakova, E. (2016). The importance of climate change and nitrogen use efficiency for future nitrous oxide emissions from agriculture. *Environmental Research Letters*, *11*(9), 094003. https://doi.org/10.1088/1748-9326/11/9/094003

Kim, D.-G., Giltrap, D., & Hernandez-Ramirez, G. (2013). Background nitrous oxide emissions in agricultural and natural lands: A meta-analysis. *Plant and Soil*, *373*(1–2), 17–30. https://doi.org/10.1007/s11104-013-1762-5

Klein Goldewijk, K., Beusen, A., Doelman, J., & Stehfest, E. (2017). Anthropogenic land use estimates for the Holocene–HYDE 3.2. *Earth System Science Data*, *9*(2), 927. https://doi.org/10.5194/essd-9-927-2017

Klein Goldewijk, K., Beusen, A., & Janssen, P. (2010). Long-term dynamic modeling of global population and built-up area in a spatially explicit way: HYDE 3.1. *The Holocene*, *20*(4), 565–573. https://doi.org/10.1177/0959683609356587

Lassaletta, L., Billen, G., Grizzetti, B., Anglade, J., & Garnier, J. (2014). 50 year trends in nitrogen use efficiency of world cropping systems: The relationship between yield and nitrogen input to cropland. *Environmental Research Letters*, *9*(10), 105011. https://doi.org/10.1088/1748-9326/9/10/105011

Leff, B., Ramankutty, N., & Foley, J. A. (2004). Geographic distribution of major crops across the world. *Global Biogeochemical Cycles*, *18*(1). https://doi.org/10.1029/2003GB002108

Li, L., Zheng, Z., Wang, W., Biederman, J. A., Xu, X., Ran, Q., et al. (2020). Terrestrial N_2O emissions and related functional genes under climate change: A global meta-analysis. *Global Change Biology*, *26*(2), 931–943. https://doi.org/10.1111/gcb.14847

Lu, C., & Tian, H. (2013). Net greenhouse gas balance in response to nitrogen enrichment: Perspectives from a coupled biogeochemical model. *Global Change Biology*, *19*(2), 571–588. https://doi.org/10.1111/gcb.12049

Lu, C., & Tian, H. (2017). Global nitrogen and phosphorus fertilizer use for agriculture production in the past half century: Shifted hot spots and nutrient imbalance. *Earth System Science Data*, *9*(1), 181. https://doi.org/10.5194/essd-9-181-2017

Mosier, A., Kroeze, C., Nevison, C., Oenema, O., Seitzinger, S., & Van Cleemput, O. (1998). Closing the global N_2O budget: Nitrous oxide emissions through the agricultural nitrogen cycle. *Nutrient Cycling in Agroecosystems*, *52*(2–3), 225–248. https://doi.org/10.1023/A:1009740530221

Myhre, G., Shindell, D., Bréon, F.-M., Collins, W., Fuglestvedt, J., Huang, J., et al. (2013). Anthropogenic and natural radiative forcing. In C. Intergovernmental Panel on Climate (Ed.), *Climate change 2013—The physical science basis: Working group I contribution to the Fifth Assessment Report of the Intergovernmental Panel on Climate Change* (pp. 659–740). Cambridge: Cambridge University Press.

Nevison, C., & Holland, E. (1997). A reexamination of the impact of anthropogenically fixed nitrogen on atmospheric N_2O and the stratospheric O_3 layer. *Journal of Geophysical Research*, *102*(D21), 25,519–25,536. https://doi.org/10.1029/97JD02391

Nishina, K., Ito, A., Hanasaki, N., & Hayashi, S. (2017). Reconstruction of spatially detailed global map of NH_4^+ and NO_3^- application in synthetic nitrogen fertilizer. *Earth System Science Data*, *9*(1), 149. https://doi.org/10.5194/essd-9-149-2017

Olivier, J. G., JJm, B., Peters, J. A., Bakker, J., Visschedijk, A. J., & Bloos, J. J. (2002). Applications of EDGAR emission database for global atmospheric research. Global Change NOP-NRP report 410200051 RIVM rapport 773301001.

Pan, S., Tian, H., Dangal, S. R., Yang, Q., Yang, J., Lu, C., et al. (2015). Responses of global terrestrial evapotranspiration to climate change and increasing atmospheric CO_2 in the 21st century. *Earth's Future*, *3*(1), 15–35. https://doi.org/10.1002/2014EF000263

Pan, S., Tian, H., Dangal, S. R., Zhang, C., Yang, J., Tao, B., et al. (2014). Complex spatiotemporal responses of global terrestrial primary production to climate change and increasing atmospheric CO_2 in the 21st century. *PLoS ONE*, *9*(11), e112810. https://doi.org/10.1371/journal.pone.0112810, https://doi.org/10.1371/journal.pone.0112810

Pärn, J., Verhoeven, J. T., Butterbach-Bahl, K., Dise, N. B., Ullah, S., Aasa, A., et al. (2018). Nitrogen-rich organic soils under warm well-drained conditions are global nitrous oxide emission hotspots. *Nature Communications*, *9*(1), 1135. https://doi.org/10.1038/s41467-018-03540-1

Prather, M. J., Hsu, J., DeLuca, N. M., Jackman, C. H., Oman, L. D., Douglass, A. R., et al. (2015). Measuring and modeling the lifetime of nitrous oxide including its variability. *Journal of Geophysical Research: Atmospheres*, *120*, 5693–5705. https://doi.org/10.1002/2015JD023267

Prinn, R. G., Weiss, R. F., Arduini, J., Arnold, T., DeWitt, H. L., Fraser, P. J., et al. (2018). History of chemically and radiatively important atmospheric gases from the advanced global atmospheric gases experiment (AGAGE). *Earth System Science Data*, *10*(2), 985–1018. https://doi.org/10.5194/essd-10-985-2018

Rapson, T. D., & Dacres, H. (2014). Analytical techniques for measuring nitrous oxide. *TrAC Trends in Analytical Chemistry*, *54*, 65–74. https://doi.org/10.1016/j.trac.2013.11.004

Reay, D. S., Davidson, E. A., Smith, K. A., Smith, P., Melillo, J. M., Dentener, F., & Crutzen, P. J. (2012). Global agriculture and nitrous oxide emissions. *Nature Climate Change*, *2*(6), 410–416. https://doi.org/10.1038/nclimate1458

Ren, W., Banger, K., Tao, B., Yang, J., Huang, Y., & Tian, H. (2020). Global pattern and change of cropland soil organic carbon during 1901–2010: Roles of climate, atmospheric chemistry, land use and management. *Geography and Sustainability*. https://doi.org/10.1016/j.geosus.2020.03.001

Ren, W., Tian, H., Xu, X., Liu, M., Lu, C., Chen, G., et al. (2011). Spatial and temporal patterns of CO_2 and CH_4 fluxes in China's croplands in response to multifactor environmental changes. *Tellus B*, *63*(2), 222–240. https://doi.org/10.1111/j.1600-0889.2010.00522.x

Reynolds, C., Jackson, T., & Rawls, W. (2000). Estimating soil water-holding capacities by linking the Food and Agriculture Organization soil map of the world with global pedon databases and continuous pedotransfer functions. *Water Resources Research*, *36*(12), 3653–3662. https://doi.org/10.1029/2000WR900130

Reynolds, J. F., & Acock, B. (1997). Modularity and genericness in plant and ecosystem models. *Ecological Modelling*, *94*(1), 7–16. https://doi.org/10.1016/S0304-3800(96)01924-2

Ri, X., & Prentice, I. C. (2008). Terrestrial nitrogen cycle simulation with a dynamic global vegetation model. *Global Change Biology*, *14*(8), 1745–1764. https://doi.org/10.1111/j.1365-2486.2008.01625.x

Rice, C. W., & Smith, M. S. (1982). Denitrification in no-till and plowed soils. *Soil Science Society of America Journal*, *46*(6), 1168–1173. https://doi.org/10.2136/sssaj1982.03615995004600060010x

Rowlings, D., Grace, P., Scheer, C., & Liu, S. (2015). Rainfall variability drives interannual variation in N_2O emissions from a humid subtropical pasture. *Science of the Total Environment*, *512*, 8–18. https://doi.org/10.1016/j.scitotenv.2015.01.011

Saikawa, E., Prinn, R., Dlugokencky, E., Ishijima, K., Dutton, G., Hall, B., et al. (2014). Global and regional emissions estimates for N_2O. *Atmospheric Chemistry and Physics*, *14*(9), 4617–4641. https://doi.org/10.5194/acp-14-4617-2014

Shcherbak, I., Millar, N., & Robertson, G. P. (2014). Global metaanalysis of the nonlinear response of soil nitrous oxide (N_2O) emissions to fertilizer nitrogen. *Proceedings of the National Academy of Sciences*, *111*(25), 9199–9204. https://doi.org/10.1073/pnas.1322434111

Smith, K. A., Mosier, A. R., Crutzen, P. J., & Winiwarter, W. (2012). The role of N_2O derived from crop-based biofuels, and from agriculture in general, in Earth's climate. *Philosophical Transactions of the Royal Society of London B: Biological Sciences*, *367*(1593), 1169–1174. https://doi.org/10.1098/rstb.2011.0313

Stehfest, E., & Bouwman, L. (2006). N_2O and NO emission from agricultural fields and soils under natural vegetation: Summarizing available measurement data and modeling of global annual emissions. *Nutrient Cycling in Agroecosystems*, *74*(3), 207–228. https://doi.org/10.1007/s10705-006-9000-7

Syakila, A., & Kroeze, C. (2011). The global nitrous oxide budget revisited. *Greenhouse Gas Measurement and Management*, *1*(1), 17–26. https://doi.org/10.3763/ghgmm.2010.0007

Tao, B., Tian, H., Ren, W., Yang, J., Yang, Q., He, R., et al. (2014). Increasing Mississippi river discharge throughout the 21st century influenced by changes in climate, land use and atmospheric CO_2. *Geophysical Research Letters*, *41*, 4978–4986. https://doi.org/10.1002/2014GL060361

Thompson, R. L., Lassaletta, P. K. P., Wilson, C., Wells, K. C., Gressent, A., Koffi, E. N., et al. (2019). Acceleration of global N_2O emissions seen from two decades of atmospheric inversion. *Nature Climate Change*, *9*, 993–998. https://doi.org/10.1038/s41558-019-0613-7

Tian, H., Lu, C., Ciais, P., Michalak, A. M., Canadell, J. G., Saikawa, E., et al. (2016). The terrestrial biosphere as a net source of greenhouse gases to the atmosphere. *Nature*, *531*(7593), 225–228. https://doi.org/10.1038/nature16946

Tian, H., Lu, C., Melillo, J., Ren, W., Huang, Y., Xu, X., et al. (2012). Food benefit and climate warming potential of nitrogen fertilizer uses in China. *Environmental Research Letters*, *7*(4), 044020. https://doi.org/10.1088/1748-9326/7/4/044020

Tian, H., Xu, R., Pan, S., Yao, Y., Bian, Z., Cai, W. J., et al. (2020). Long-term trajectory of nitrogen loading and delivery from Mississippi River Basin to the Gulf of Mexico. *Global Biogeochemical Cycles*, *34*, e2019GB006475. https://doi.org/10.1029/2019GB006475

Tian, H., Xu, X., Liu, M., Ren, W., Zhang, C., Chen, G., & Lu, C. (2010). Spatial and temporal patterns of CH_4 and N_2O fluxes in terrestrial ecosystems of North America during 1979–2008: Application of a global biogeochemistry model. *Biogeosciences*, *7*(9), 2673–2694. https://doi.org/10.5194/bg-7-2673-2010

Tian, H., Xu, X., Lu, C., Liu, M., Ren, W., Chen, G., et al. (2011). Net exchanges of CO_2, CH_4, and N_2O between China's terrestrial ecosystems and the atmosphere and their contributions to global climate warming. *Journal of Geophysical Research*, *116*, G02011. https://doi.org/10.1029/2010JG001393

Tian, H. Q., Yang, J., Lu, C., Xu, R., Canadell, J. G., Jackson, R. B., et al. (2018). The global N_2O model intercomparison project. *Bulletin of the American Meteorological Society*, *99*(6), 1231–1252. https://doi.org/10.1175/BAMS-D-17-0212.1

Tian, H. Q., Yang, J., Xu, R., Lu, C., Canadell, J. G., Davidson, E. A., et al. (2019). Global soil nitrous oxide emissions since the preindustrial era estimated by an ensemble of terrestrial biosphere models: Magnitude, attribution, and uncertainty. *Global Change Biology*, *25*, 640–659. https://doi.org/10.1111/gcb.14514

Tian, H. Q., Xu, R., Canadell, J. G., Thompson, R. L., Winiwarter, W., Suntharalingam, P., et al. (2020). A comprehensive quantification of global nitrous oxide sources and sinks. *Nature*, *586*, 248–258. https://doi.org/10.1038/s41586-020-2780-0

van Aardenne, J. A., Dentener, F. J., Olivier, J. G. J., Goldewijk, C. G. M. K., & Lelieveld, J. (2001). A 1°×1° resolution data set of historical anthropogenic trace gas emissions for the period 1890–1990. *Global Biogeochemical Cycles*, *15*(4), 909–928. https://doi.org/10.1029/2000GB001265

Van Groenigen, K. J., Osenberg, C. W., & Hungate, B. A. (2011). Increased soil emissions of potent greenhouse gases under increased atmospheric CO_2. *Nature*, *475*(7355), 214–216. https://doi.org/10.1038/nature10176

Wang, Q., Zhou, F., Shang, Z., Ciais, P., Winiwarter, W., Jackson, R. B., et al. (2020). Data-driven estimates of global nitrous oxide emissions from croplands. *National Science Review*, *7*(2), 441–452. https://doi.org/10.1093/nsr/nwz087

Wei, Y., Liu, S., Huntzinger, D. N., Michalak, A., Viovy, N., Post, W., et al. (2014). The North American carbon program multi-scale synthesis and terrestrial model intercomparison project–part 2: Environmental driver data. *Geoscientific Model Development*, *7*(6), 2875–2893. https://doi.org/10.5194/gmd-7-2875-2014

Wrage-Mönnig, N., Horn, M. A., Well, R., Müller, C., Velthof, G., & Oenema, O. (2018). The role of nitrifier denitrification in the production of nitrous oxide revisited. *Soil Biology and Biochemistry*, *123*, A3–A16. https://doi.org/10.1016/j.soilbio.2018.03.020

Xu, R., Pan, S., Chen, J., Chen, G., Yang, J., Dangal, S., et al. (2018). Half-century ammonia emissions from agricultural systems in Southern Asia: Magnitude, spatiotemporal patterns, and implications for human health. *Geo Health*, *2*(1), 40–53. https://doi.org/10.1002/2017GH000098

Xu, R., Tian, H., Lu, C., Pan, S., Chen, J., Yang, J., & Bowen, Z. (2017). Preindustrial nitrous oxide emissions from the land biosphere estimated by using a global biogeochemistry model. *Climate of the Past*, *13*(7), 977–990. https://doi.org/10.5194/cp-13-977-2017

Xu, R., Tian, H., Pan, S., Prior, S. A., Feng, Y., Batchelor, W. D., et al. (2019). Global ammonia emissions from synthetic nitrogen fertilizer applications in agricultural systems: Empirical and process-based estimates and uncertainty. *Global Change Biology*. https://doi.org/10.1111/gcb.14499

Yan, X., Akimoto, H., & Ohara, T. (2003). Estimation of nitrous oxide, nitric oxide and ammonia emissions from croplands in East, Southeast and South Asia. *Global Change Biology*, *9*(7), 1080–1096. https://doi.org/10.1046/j.1365-2486.2003.00649.x

Yang, Q., Tian, H., Friedrichs, M. A., Hopkinson, C. S., Lu, C., & Najjar, R. G. (2015). Increased nitrogen export from eastern North America to the Atlantic Ocean due to climatic and anthropogenic changes during 1901–2008. *Journal of Geophysical Research: Biogeosciences*, *120*, 1046–1068. https://doi.org/10.1002/2014JG002763

Yao, Y., Tian, H., Shi, H., Pan, S., Xu, R., Pan, N., & Canadell, J. G. (2020). Increased global nitrous oxide emissions from streams and rivers in the Anthropocene. *Nature Climate Change*, *10*(2), 138–142. https://doi.org/10.1038/s41558-019-0665-8

Zaehle, S., Ciais, P., Friend, A. D., & Prieur, V. (2011). Carbon benefits of anthropogenic reactive nitrogen offset by nitrous oxide emissions. *Nature Geoscience*, *4*(9), 601–605. https://doi.org/10.1038/ngeo1207

Zhang, B., Tian, H., Lu, C., Dangal, S. R., Yang, J., & Pan, S. (2017). Global manure nitrogen production and application in cropland during 1860–2014: A 5 arcmin gridded global dataset for Earth system modeling. *Earth System Science Data*, *9*(2). https://doi.org/10.5194/essd-9-667-2017

Zhang, B., Tian, H., Ren, W., Tao, B., Lu, C., Yang, J., et al. (2016). Methane emissions from global rice fields: Magnitude, spatiotemporal patterns, and environmental controls. *Global Biogeochemical Cycles*, *30*, 1246–1263. https://doi.org/10.1002/2016GB005381

Zhang, J., Tian, H., Yang, J., & Pan, S. (2018). Improving representation of crop growth and yield in the dynamic land ecosystem model and its application to China. *Journal of Advances in Modeling Earth Systems*, *10*, 1680–1707. https://doi.org/10.1029/2017MS001253

Zhou, F., Shang, Z., Zeng, Z., Piao, S., Ciais, P., Raymond, P. A., et al. (2015). New model for capturing the variations of fertilizer-induced emission factors of N_2O. *Global Biogeochemical Cycles*, *29*, 885–897. https://doi.org/10.1002/2014GB005046